Chemosensitization of doxorubicin against lung cancer by nature borneol, involvement of TRPM8-regulated calcium mobilization

Haoqiang Lai
Jinan University
Chang Liu
Jinan University Institute for Economic and Social Research
Wenwei Lin
Jinan University
tf Chen (felixchentf@gmail.com)
Jinan University
An Hong
Jinan University

Research

Keywords: Natural Borneol, DOX, TRPM8, Synergism, Calcium mobilization, Non-small cell lung cancer

Posted Date: February 24th, 2020

DOI: https://doi.org/10.21203/rs.2.24354/v1

Abstract

Background

Lung cancer possesses high mortality rate and tolerances to multiple chemotherapeutics. Natural Borneol (NB) is a monoterpenoid compound that found to facilitate the bioavailability of drugs. In this study, we attempted to investigate effects of NB on the chemosensitivity in A549 cells and try to elucidate its therapeutic target.

Methods

The effects of NB on chemosensitivity in A549 cells was examined by MTT assay. The mechanism studies were evaluated by flow cytometry and western blotting assay. Surface plasmon resonance (SPR) and LC-MS combined analysis (MS-SPRi) was performed to elucidate the candidate target of NB contributes to this synergism. The chemosensitizing capacity of NB in vivo was conducted in nude mice bearing A549 tumors.

Results

NB pretreatment sensitizes A549 cells to low dosage of DOX, leading to a 15.7% to 41.5% increase in apoptosis, which is corelated with ERK and AKT inactivation but activation of phosphor-p38MAPK, -JNK and p53. Furthermore, this synergism depends on reactive oxygen species (ROS) generation. The MS-SPRi analysis reveals that the transient receptor potential melastatin-8 (TRPM8) is the interaction target of NB in potentiating DOX killing potency. Genetically knock down of TRPM8 significantly suppress the chemosensitizing effects of NB with the involvement of inhibiting ROS generation through restraining calcium mobilization. Moreover, pretreatment of NB synergistically enhanced the anticancer effects of DOX to delay tumor progression in vivo.

Conclusions

These results suggest that TRPM8 may be a valid therapeutic target in the potential application of NB serves as a chemosensitizer for lung cancer treatment.

Background

Non-small cell lung cancer (NSCLC), accounting for 75%-80% of lung cancer, is the leading cause of the mortality worldwide, which is higher than prostate, breast and colorectal cancers death combined[1, 2]. Despite tremendous strategies have been made for lung cancer research, the 5-year survival rate remains at 10%-13% for NSCLC patients. Thus far, except for surgical and radio therapy, chemotherapy still considered as the mainly choice in lung cancer therapy, however, the response rate of single agents in NSCLC is still lower than 15%[3]. Therefore, developing novel treatment remedies for NSCLC comes to be of extremely imperative.

Doxorubicin is widely used for solid tumors therapy, including NSCLC, due to its potent cytotoxic for a long time[4]. Studies revealed that the propose mechanism of DOX towards many malignancies is correlated with targeting topoisomerase II[5], inhibiting anti-apoptosis proteins expression[6], and inducing activation of p53[7]. However, drug-resistance greatly limited the therapeutic efficiency of DOX, especially for advanced NSCLC treatment, which may due to overexpression of multi-drug resistance proteins[8], NF-κB activation[9] and topoisomerase II activities alteration[10]. Additionally, dose limiting cardiotoxicity of DOX, higher doses induced bone marrow depression and poor drug delivery also considered as primary obstacles of therapeutic efficiency in lung cancer treatment. The combination chemotherapy has been postulated as a promising treatment strategy. Emerging evidences have disclosed the therapeutic effects of combination regimens, such as cisplatin combined with taxanes, gemcitabine[11], curcumin and 5-fluorouracil[12] for cancer treatments. Recently, clinical evidence disclosed that therapies combined with DOX and lurbinectedin significantly increased the therapeutic index with response rate of 67%. Moreover, no cross resistance with platinum drugs was observed during the treatment[13]. However, searching for more new effective agents to improve the efficacy of DOX for cancer therapy turns to be of great interest.

Natural products have been widely used in traditional medicine, and they also possess great prospects in the treatment of cancer, such as tripterygium wilfordii[14], betulinic acid[15] and triptolide[16]. Borneol, a monoterpenoid compound, has been used in antibacterial, analgesic and anti-inflammatory for 2000 years. Nowadays, accumulating studies have shown that borneol can promote the transdermal and mucosal absorption of drugs. Recently, some studies disclosed that borneol can enhance the anti-tumor effects of selenocysteine[17], curcumin[18], didemethoxycurcumin[19], cisplatin[20] and paclitaxel[9]. Although these studies have suggested the potential application prospect of borneol in cancer prevention, it is not clear whether borneol can be used to improve the therapeutic efficiency of chemotherapy in lung cancer treatment, and the candidate target of borneol in chemotherapy is remain to be authenticated. Nowadays, RNA-Seq[21] and ITRAQ[22] are widely used for exploring the targets of small molecules, proteins and peptides. However, these strategies are still unable to reflect the direct interaction between protein targets and drug molecules. Surface plasmon resonance (SPR) biosensor technology has been widely used to characterize unmodified biological drugs and captured macromolecular targets of small molecular agents[23, 24] due to several advantages such as samples are no needed for labeling and real time monitoring of intermolecular interaction. In this study, we are aim to explore whether borneol can enhance the inhibitory effect of DOX on the growth of non-small cell lung cancer. And the combination of SPR and LC-MS analysis (MS-SPRi) was used to elucidate the underlying target of borneol serves as chemosensitizer in chemotherapy.

Materials And Methods

Chemicals and reagents

Natural borneol (NB) was obtained from China Institute for the Control of Pharmaceutical and Biological products. Doxorubicin, 5-Fu, Cisplatin, Paclitaxel, Propidium iodide (PI), DCFH-DA, Rhodamine 123,

MitoTracker Green, bicinchoninic acid (BCA) kit and MTT were acquired from Sigma-Aldrich. DMEM and fetal bovine serum (FBS) were obtained from Invitrogen (Carlsbad, CA). Caspases substrate for caspase-3/-8/-9 were obtained from Calbiochem. Fluo-3 AM was purchased from Eugene, Oregon, USA. All antibody used in this study were purchased from Cell Signaling Technology (Beverly, MA). All the chemicals and solvents were analytically pure.

Cell Culture And Determination Of Cell Viability

A549 cells and NCM460 cells were purchased from ATCC (Manassas, VA) and cultured according to manufactory's instruction. After pretreated with NB for 12 h, different doses of chemotherapy agents were added and cocultured for 72 h. Cell viability was determined by MTT assay according to previous publications[25].

Clonogenic Assay

Cells (2000/well) were seed in 6-well plates overnight and then treated with NB for 12 h followed by Doxorubicin. After 24 h, the culture condition was changed by fresh DMEM and cells allowed to grow for 8 days. After that the cells were rinsed 3 times with PBS, 0.5% crystal violet (wt/vol) in water was used for cells staining and then captured by camera (Life technologies EVOS®FL Auto).

Cellular Uptake Of DOX

5×10^4 cells/mL of A549 cells were allowed to attach in 6-well plate overnight. Cells were treated with indicated concentration of NB for 12 h followed by DOX for 1, 2, 4, and 8 h. Cells were stained with DAPI for another 30 min. The intracellular DOX accumulation was examined by Microscope (Life technologies EVOS®FL Auto) and evaluated by using Flow cytometry assay (Beckman, CytoFLEX S).

Evaluation Of P-glycoprotein (P-gp) Functional

A549 cells were incubated with indicated concentration of NB for different times. Then, 5 μM Rhodamine123 was added and co-incubated for 1 h at 37°C. The intracellular fluorescence intensity was recorded with ex at 488 nm and em at 530 nm after cells lysed with 1% Tritoon-100 PBS solution.

Flow Cytometric Analysis

Annexin-V and PI staining assay was used to evaluate the apoptosis effects induced by the combined treatment of NB and DOX as per the manufactory protocol. The apoptosis cells were collected and recorded by CytoFLEX S (Beckman). As for cell cycle distribution analysis. Cells were collected and fixed with 70% cold ethanol overnight. Cells were collected by centrifugation and then stained with PI for 30 min in dark or stained with Hoechst 33342 for 30 min. After that flow cytometry assay was used to analysis the distribution of cell cycle and ModFit 5.0 software was used to analysis the results.

Evaluation Of Mitochondrial Structure And Mitochondrial Electric Potential (Δψ)

MitoTracker Green CMXRos and DAPI were exploited to determine the structure of mitochondria according to the protocols. The structure of mitochondria was examined under a fluorescent microscope (Life technologies EVOS®FL Auto, 100×). Mitochondria electric potential (Δψ) examination was performed according to previously described[26]. The fluorescence intensity was recorded by using Biotek Microplate System with ex at 550 nm and em at 600 nm for red fluorescence, and ex at 485 nm and em at 535 nm for green fluorescence.

ROS Generation Examination

DCFH-DA fluorescence assay was used to examine the intracellular ROS accumulation. Briefly, cells were stained with DCFH-DA fluorescence probe for 30 min and then washed with PBS twice to remove the unlabeled probe. Then 10^6 cells per well were incubated with NB and DOX for 2 h, and the changes of fluorescence intensity were recorded by Biotek Microplate System with ex at 488 nm and em at 525 nm. The relative fluorescence intensity of treated cells was expressed as percentage of control (as 100%).

Caspase Activity Assay

Caspases specific substrates were used to evaluate the activation of caspases induced by NB and DOX. Briefly, 100 μg/well protein was incubated with caspase substrates at 37 ℃ for 2 h. The fluorescence intensity was recorded by Biotek Microplate System with ex at 380 nm and em at 440 nm.

Screening and identification of captured proteins of NB in A549 cells

To further elucidate the targeting protein of NB in A549 cells, MS-SPRi were exploited. Briefly, total cellular proteins of A549 cells were extracted by incubating cells in lysis buffer and flowed through the nanosensor chip (Betterways Inc., China) immobilized by NB. The captured proteins or peptides by NB were digested in situ by trypsin, and then identified with HPLC-MS/MS. MaxQuant software (COX LAB, version 1.3.0.5) was applied for MS data analysis. The captured peptides and proteins were analysed through using Proteome Discoverer (Thermo Fisher Scientific, version 1.7) by retrieving in UniProtKB/Swiss-Prot.

siRNA Transfection

The siRNA duplexes were obtained from sangon biotech and the siRNA sequences were presented as follows: TRPM8, sense (5’-3’) GGATGCTGATCGATGTGTT; antisense (5’-3’) AACACAUCGAUCAGCAUCCTT; Androgen receptor (AR), sense (5’-3’) GAGCACTGAAGATACTGCTGA; antisense (5’-3’) ACGUGACACGUUCGGAGAATT. Transfection of siRNA oligonucleotides was carried out as per the manufacturer’s protocol (Invitrogen). After transfection for 48 h, cells were pretreated with 160 μg/mL NB for 12 h followed by 0.25 μM DOX for 48 h. Meanwhile the siRNA control was carried out as the same procedure. Finally, cell viability was evaluated by using MTT assay.

Evaluation Of Intracellular Ca^{2+} Mobilization

Intracellular calcium mobilization of A549 cells evoked by NB was performed using flow cytometry assay. Briefly, after loaded with 5 μM of Fluo-3 acetomethyl ester (Eugene, Oregon, USA), the cells (0.3×10^6 cells/tube) were collected for 20 s to acquire baseline fluo-3 fluorescence. Then, indicated concentration of NB was quickly added and the changes of green fluorescence was recorded by setting up the stop-time condition at 120–200 s.

Western Blot Analysis

Changes of different protein-induced by NB and DOX were evaluated by employing western blotting assay.

In vivo antitumor activity

The animal experiment was approved by the Animal Experimentation Ethics Committee. About 1×10^6 A549 cells in PBS were subcutaneously injected into the right oxter of nude mice. After the tumor volume reached to 50–60 mm^3, mice were randomly divided into 6 groups (8 mice/group) for control group, i.v.DOX, i.v.NB, p.o.NB, i.v.NB + i.v.DOX and p.o.NB + i.v.DOX. The selected intravenous dosage of NB (0.002 g/kg), oral dosage of NB (0.2 g/kg) and intravenous dosage of DOX (0.004 g/kg) was carried out according to previously described[27–29]. Mice were euthanized and the tumor tissues were harvested, photographed, and weighted at the end of the experiments. Meanwhile, serum from the venous blood of each groups were harvested and applied for serum clinical chemistry analysis.

Extraction Of DOX From Tumor Tissues

DOX from tumor tissues was extracted as previously described[30]. The fluorescence intensity examination with the excitation and emission wavelengths set at ex = 470 nm and em = 595 nm. Meanwhile, the stander curve was carried out as the same procedure with the DOX concentration varied form 0.025, 0.05, 0.5, 1.0, 5.0, 10 μg/mL.

Statistical analysis

All experiments were performed three independent repeats. Data were expressed as mean ± S.D. Statistical analysis was performed using SPSS statistical package (SPSS, Inc. Chicago, IL). * and ** are denoted as statistically significant.

Results

NB potentiates cytotoxicity of DOX against A549 cells through enhancing cellular uptake

Firstly, the acute toxicity of borneol was examined. As illustrated in Table. s1, the median lethal dose (LD_{50}) of synthetic borneol (SB) was 3129 mg/kg and the 95% confidence interval at 1750 ~ 5000 mg/kg, while 5000 mg/kg and 2016 ~ 9810 mg/kg were found in NB, respectively. Moreover, significant pathology changes were found in liver, spleen and lung only in SB (5000 mg/kg) treatment mice, while

slightly inflammation effects were found in stomach and intestinum tenue in both SB and NB (5000 mg/kg) treated mice (Fig. s1). These results suggest that NB exhibits higher safety index than SB, thus NB was selected for chemo-sensitizing study. As illustrated in Table s2, NB was able to enhance the cytotoxic effects of DOX against A549 cells with the IC_{50} value of DOX decreased to 0.18 ± 0.06 μM. Similar enhancive effects of NB on 5-FU, paclitaxel and cisplatin were also observed. These results suggest the sensitizing capacity of NB on chemotherapeutic agents against A549 cells, and we selected NB and DOX for further study. As shown in Fig. 1a, DOX treatment alone slightly restrained the A549 cells growth at the concentration range from 0.06 μM to 0.25 μM. However, strongly cytotoxicity effects were observed when cells pretreated with NB for 12 h followed by low dose of DOX for 72 h with suppression ratio increased up to 40.26%. The long term clonogenic assay also confirmed these results (Fig. 1b and 1c). Furthermore, we also explore the cytotoxicity of NB and DOX towards normal colonic NCM-460 cells. We found that NCM-460 cells were less inhibited as compared to A549 cells, which indicated that NB potentiated DOX induced prominent cells survival reduction mainly in tumor cells (Fig. 1d).

In order to investigate the underlying mechanism of the cytotoxicity effects induced by NB and DOX, the intracellular accumulation of DOX was examined. As illustrated in Fig. 1g, NB pretreatment dramatically augment the intracellular accumulation of DOX when compared to DOX treatment alone as evidenced by more remarkable red fluorescence, which is in accordance with the FACS data in Fig. 1e and 1 f. Moreover, drug resistance mediated by P-glycoprotein (P-gp) also confirmed to be one of the major causes of DOX-resistance in NSCLC[31]. Therefore, P-gp functional analysis was also conducted. As shown in Fig. 1g and 1 h, NB was able to restrain the P-gp action in a time and dose-dependent manner as indicated by the increased intracellular fluorescence intensity of rhodamine 123. Together, these results demonstrate that NB inhibits P-gp function to potentiates the cytotoxic effects of DOX against A549 cells.

NB synergizes with DOX to induce apoptosis through activating caspases cascade in A549 cells

We next employed Flow cytometry assay to examine the mode of cell death triggered by this combination treatment. As depicted in Fig. 2a and 2b, no significant cycle distribution changes were observed in NB treatment groups, while significant accumulated population of Sub-G1 (17.05%) and G0/G1 phase were observed after DOX incubation, which suggests that DOX is able to trigger both cell cycle arrest and apoptosis in A549 cells. However, significant apoptosis effects were observed in cells that pretreated with NB followed by DOX, as illustrated by the increased population of Annexin V and PI double positive cells in Fig. 2c. For instance, 6.16% apoptosis cells were observed in NB treatment alone, while 15.7% was found in DOX incubation groups. However, NB pretreatment significantly enhanced the killing potency of DOX with the apoptosis proportion increased to 41.5%, which is further confirmed by the morphology changes of treated cells (Fig. 2d). These results indicate that NB sensitizes A549 cells to DOX-mediated killing potency by inducing apoptosis.

In order to further confirm the apoptosis inducing effects of NB combined with DOX, fluorometric assay to examine caspases activation was examined. As demonstrated in Fig. 2e and 2f, both NB and DOX were able to induce slight activation of caspase-3/-8/-9. However, cells pretreated with NB followed by the

incubation of DOX were found to synergistically increased the activation of caspase-3/-8/-9, which indicates the activation of extrinsic and intrinsic apoptosis pathways. The western blotting assay results of significant cleavage of caspase-9, caspase-8, caspase-3, and PARP further strengthens these findings. Together, these results demonstrate that NB enhances DOX-induced A549 cells death mainly by inducing apoptosis through activating extrinsic and intrinsic apoptosis pathways.

Activation of ROS-mediated pathway contributes to the apoptosis effects induced by NB and DOX

Extrinsic and intrinsic apoptosis signal will converge to mitochondria. Therefore, MitoTracker Green probe was used to examine the integrity of mitochondria. The results show that compared to the extensively interconnected and filamentous appearing network of mitochondria observed in the control treatment, NB slightly triggered mitochondria structure damage after 8 h incubation. Meanwhile, slightly destroyed structure can be observed after cells treated with DOX alone for 4 h. However, small fragmentation of mitochondria was observed early at 2 h after the combined incubation of NB and DOX, and followed by notable damage at 4 h, and became progressively worse at 8 h (Fig. 3a). The depleted mitochondrial membrane potential ($\Delta\psi m$) also confirmed the damage of mitochondria (Fig. s2). Furthermore, we found that Bcl-2 expression was strongly inhibited by the combined treatment of NB and DOX, while the expression of tBid and Bax was significantly upregulated (Fig. 3b). These results suggest that NB synergized the killing potency of DOX is highly correlated with mitochondria dysfunction.

Triggering DNA damage has been found to be one of the major mechanisms of DOX[32], which may regulate mitochondria-mediated apoptosis through activating p53. In this study, we found that NB significantly enhanced DOX-induced DNA damage, as evidenced by the upregulated protein expression level of phosphorylated ATM, ATR and histone (Ser 139), as well as phosphorylated p53 (Ser 15) (Fig. 3c). These results indicate that DNA damage-mediated p53 activation contributes to the sensitizing effects of NB on DOX in A549 cells.

Mitogen-activated protein kinase (MAPK) and phosphoinositide 3-kinase (PI3K)/AKT pathways paly important role in the proliferation and metastasis of cancer cells. We next evaluate whether the combination treatment of NB and DOX could affect the function of these kinases. As depicted in Fig. 3d and 3e, NB and DOX combined treatment dramatically suppressed phosphorylated-AKT and phosphorylated-ERK while upregulated the phosphorylation of p38 MAPK (Thr180/Tyr182) and SAPK/JNK (Thr183/Tyr185). These results suggest that NB synergizes with DOX induces A549 cells apoptosis through inhibiting AKT and ERK activation, but stimulating p38MAPK and JNK activation.

Expanding evidences have disclosed the pivotal role of ROS in the anticancer mechanisms of DOX[33]. And ROS exhibits regulation role in the modulation of Mitogen-activated protein kinase (MAPK) and phosphoinositide 3-kinase (PI3K)/AKT pathways[34]. As shown in Fig. 3f, both NB and DOX were able to trigger ROS generation, however, strongly upregulation of ROS accumulation was achieved when cells incubated with the combined treatment of NB and DOX. Moreover, N-acetyl-L-cysteine (NAC), a thiol reducing antioxidant, pretreatment significantly inhibited cells growth suppression and cell apoptosis induced by the combined incubation of NB and DOX (Fig. 3g and 3 h), which suggested the upstream role

of ROS. Taken together, these results demonstrate that NB dramatically augments DOX-triggered cells apoptosis is relied on activation of ROS-mediated DNA pathway.

NB enhances the chemosensitivity of A549 cells to DOX through targeting TRPM8

SPR biosensor technology is widely used for peptide screening and small molecule drugs screening[35]. Since NB enhances the anticancer activities of DOX, MS-SPRi technology was exploited to elucidate the candidate targets of NB (Fig. 4a). The MS score is used to evaluate the binding strength of NB on proteins, and Peptide Spectrum Matches (PSMs) is represented as the number of peptide map matches. As shown in Fig. 4b and 4c, 31 cell lysis proteins of A549 cells were captured by NB. From Gene Ontology cluster analysis in Biological Process, we found that most of these captured proteins are involved in cellular process regulation (Fig. 4d). Additionally, 19 of 31 proteins are found to take part in the regulation of stress response. And 21% of these 19 proteins are belong to ion channel proteins, such as GABRA5, TRPM8, TRPA1 and TRPV3 (Fig. 4e and 4f). The MS score of GABRA5 (PSMs = 66) is found to be highest and followed by TRPM8 (PSMs = 31). Since GABRA5 mainly participates in neuron-neuron synaptic transmission regulation [36]. We speculate that TRPM8 may be an important target of NB, and TRPM8 was selected for further study.

TRPM8 has been considered as a cancer marker of lung cancer[37]. Lung adenocarcinoma is found to overexpress of TRPM8, and its expression is negatively correlated with the survival rate of patients according to TCGA and PROGgene database (Fig. 4g and 4 h)[38, 39], which suggests that targeting TRPM8 may help to improve the therapeutic index of lung cancer treatment. TRPM8 is an important calcium channel protein[40]. Therefore, we first detected whether NB could affect intracellular dissociative calcium concentration in A549 cells. As shown in Fig. 4i, the intracellular fluorescence signal of A549 cells loaded with Fluo-3AM probe was enhanced after NB addition and the signal was upregulated in according with the increased concentration of NB, indicating the capacity of NB in inducing calcium mobilization. In order to further investigate whether NB affects calcium accumulation through interacting with TRPM8, short interference double-stranded RNA (siRNAs) of TRPM8 interference assay was employed. As shown in Fig. 4j and 4 k, the protein expression level of TRPM8 was dramatically inhibited after 48 h transfection. The intracellular calcium signal induced by NB was significantly downregulated in the TRPM8 knock down cells when compared with siNC control groups (Fig. 4l). These results further indicate the important role of TRPM8 in calcium immobilization triggered by NB stimulation. Furthermore, we also found that knock down of TRPM8 restrained the accumulation of intracellular ROS (Fig. 4m and 4n) induced by NB combined with DOX and reversed the killing capacity of DOX against A549 cells sensitized by NB (Fig. 4o).

Except for TRPM8, we found that the MS score of androgen receptor (AR) was 1077.15 and the PSMs was 93, which indicated that AR may also participate in the sensitizing effects of NB. Furthermore, patients with high expression level of AR is also found to possess lower survival rate[39]. Therefore, in order to evaluate whether the synergistic effects of NB and DOX was relied on the interaction of NB on AR, AR knock down assay was also employed. As shown in Fig. s3, no significant changes of anticancer

effects triggered by NB and DOX were observed between siAR knock down groups and siNC control groups. This suggests that AR may not participate in the regulation of NB as a DOX sensitizer. Taken together, these results suggest that NB may synergize with DOX to achieve potent anticancer efficiency through triggering intracellular Ca^{2+} mobilization by interacting with TRPM8.

NB augments the antitumor activities of DOX in vivo.

To further evaluate the potential therapeutic efficacy of NB and DOX, we exploited xenografts nude mice model assay. As shown in Fig. 5a-5c, both borneol and DOX were found to inhibit tumor growth. After 15 days treatment, the tumor volume decreased to 268.45 mm^3 ± 17.01, and the tumor inhibition rate was 39.79%. However, the tumor volume was significantly inhibited in the combined treatment of NB and DOX. For example, the average tumor volume of p.o. NB + i.v. DOX group and i.v. NB + i.v. DOX group was 205.61 mm^3 ± 17.05 and 164.42 mm^3 ± 25.03, respectively. The tumor inhibition rate was 53.95% and 63.16% (Fig. 5d). In addition, we found that intravenous injection of borneol and DOX exhibited more potent anti-tumor effect than oral administration schedule, which may be due to more potent blood bioavailability of NB after intravenous administration[27], which promoting the accumulation of DOX in the tumor site and inducing more significant anti-tumor effects. The accumulation of DOX in tumor tissues also confirmed this result. For instance, the content of DOX was 1.89 (μg/g tumor tissue) ± 0.05 in DOX treatment groups and 3.34 (μg/g tumor tissue) ± 0.69 in p.o. NB + i.v. DOX groups. However, DOX concentration in the tumor tissues of i.v. NB + i.v. DOX groups was much higher with the content at 5.27 (μg/g tumor tissue) ± 0.41 (Fig. 5e). CD34 and Ki67 expression in tumor sections also verified these findings (Fig. 5g). Moreover, no significant pathological changes in the major organs of heart, liver, spleen, lung and kidney and TG, UA, ALB, TP, LDH were found between the combined treatments groups and control groups (Fig. 5h and 5i). Taken together, these results demonstrate that NB and DOX synergized to suppress tumor growth in vivo.

Discussion

In this study, we used MS-SPRi technique to screen the potential targets of borneol on A549 cells. According to the Gene ontology analysis results, TRPM8 may be a potential target for borneol in anti-tumor application. Many studies have shown that stimulation of TRPM8 may result in calcium mobilization and subsequently result in dissipation of $\Delta\psi m$, which promotes the release of cytokine c and other contents thus activates caspase-9 and caspase-3 to induce apoptosis. Herein, we found that borneol could induce intracellular calcium accumulation in A549 cells in a dose-dependent manner. Moreover, knock down of TRPM8 restrains the accumulation of calcium, which suggests the pivotal role of TRPM8 in calcium mobilization triggered by NB. Additionally, we also found that borneol was able to induce mitochondrial breakage, up-regulate Bax, tBiD expression and trigger mild apoptosis (the proportion of apoptosis was 6.16%), which may due to the regulation of calcium induced by borneol.

Tremendous evidences demonstrate that triggering extrinsic and intrinsic apoptosis pathway was involved in the anticancer activities of DOX[41]. The extrinsic apoptosis signal may converge to

mitochondria through translocating truncation Bid [42]. The integration of mitochondria membrane is regulated by the balance of pro-survival proteins, such as Bcl-2 and Bcl-xL, and pro-apoptosis protein, such as Bax and Bad. Upon apoptosis inducing signal transduction, $\triangle\psi m$ is depleted and ultimately result in destruction of mitochondria structure[43]. This study shows that borneol combined with DOX dramatically downregulates Bcl-2/Bax protein expression to induce mitochondrial dysfunction and activate endogenous apoptosis pathway, which suggests that mitochondria-mediated pathway exhibits an important role in NB serves as a sensitizer of DOX.

ROS has been confirmed to play important regulation roles in apoptosis, and mitochondria remains to be the potential source of ROS. In this study, we found that both DOX and borneol could induce intracellular ROS production, however, significant accumulation of ROS was observed when NB combined with DOX. This is consistent with the results of mitochondrial structural damage, membrane potential dissipation and up-regulation of pro-apoptotic protein expression induced by the combined treatment groups. Furthermore, NAC could effectively inhibit this synergistic effect, indicating the importance of ROS in this synergism. Moreover, the intracellular ROS production induced the combined treatment was significantly attenuated after the knocked down of TRPM8, which further suggest the important role of TRPM8 in ROS overproduction-mediated apoptosis induced by NB combined with DOX.

The activation of p42/44MAPK (ERK1/2) and AKT signaling pathways have been considered to be an important feature of tumor proliferation and invasion. Calcium signaling is involved in regulating p44/p42-MAPK pathway and PI3K-AKT-mTOR signaling pathway[44, 45]. Similar to ROS, when the intracellular calcium exceeds a certain threshold, it may in turn inhibit the p44/p42-MAPK pathway leading to crosstalk between other signaling pathways. In addition, studies have shown that MAPK and AKT are the main oxidative stress sensitive signal transduction pathways [25]. Consistent with reported studies, we found that DOX can activate p38MAPK and JNK signals[46]. We found that both borneol and DOX could inhibit the expression of phosphate ERK1/2, borneol and DOX exhibit a synergistic inhibitory effect on the expression of phosphorylated AKT and ERK1/2. In addition, borneol combined with DOX induced more significant expression of phosphorylated p38MAPK and phosphorylated JNK. The underlying mechanism may be that borneol stimulates the release of calcium ions through interacting with TRPM8, which resulting in the translocation of Ca^{2+} to mitochondria and induces mitochondrial damage and leading to ROS production. ROS modulates MAPK, AKT signal transduction and enhances the therapeutic effects of DOX.

Cellular overproduction of ROS may result in oxidation of protein, lipid and DNA damage. In response to DNA damage, downstream molecules such as ATM and ATR can be recruited and activated, which result in activation of p53 and ultimately inducing Bax, PUMA, Noxa and Bid expression [47]. Strategy that targeted and activated p53 considered as important event for sensitization treatment. DOX is a potent apoptosis-induced chemotherapeutic agent that correlated with DNA damage, ROS generation and activation of p53[48]. We found that NB sensitized A549 cells to DOX-mediated killing through inducing DNA damage thus activated p53 signal pathway. Furthermore, this synergism in dependent on ROS generation, which suggest the critical role of ROS in this synergism.

In this study, we found that the proteins captured by borneol such as AR and RFA1 have relatively high MS scores and abundance on chips (PSMs). Additionally, AR and RFAI have been confirmed to be closely related to the development of cancer, such as lung cancer, prostate cancer, liver cancer and breast cancer[39]. Data from TCGA database show that RFA1 in human lung cancer tissue is in a state of high expression (P = 1.09E-06) [39], which rendered it as a therapeutic target for lung cancer treatment[50]. In this study, we found that the cell cycle distribution of A549 cells did not change significantly after the treatment of borneol, and no significant changes of the expression of RFAI in A549 cells (data are not shown), which indicates that borneol may not change the biological function of RFAI. Similarly, the killing effect of borneol combined with DOX on A549 cells did not affected after knock down of AR (Fig. s3). These results suggest that borneol may not enhance the anti-tumor activity of DOX by inhibiting the activity of RFA1 and AR.

Conclusion

Taken together, this study demonstrates that NB is able to augment the therapeutic effects of DOX in vitro and in vivo with the involvement of TRPM8-regulated calcium mobilization. Therefore, we propose that NB suppresses the biological functional of multidrug resistance proteins P-gp and enhances the cellular uptake of DOX, which augments DNA damage-mediated p53 activation and thus induces mitochondria dysfunction and promotes apoptosis. Additionally, NB evokes Ca^{2+} signals and facilitates mitochondria dysfunction, which promotes the release of ROS and induces inactivation of ERK1/2 and AKT but activation of JNK and p38MAPK to boost up p53-mediated apoptosis pathway (Fig. 6). Together, these results suggest that NB may be developed as a potential chemosensitizer to improve the efficacy of DOX-based cancer therapy for the treatment of lung cancer.

Abbreviations

NB: natural borneol; SB: synthetic borneol; MS-SPRi: Surface plasmon resonance (SPR) and LC-MS combined analysis; ROS: reactive oxygen species; TRPM8: transient receptor potential melastatin-8; NSCLC: Non-small cell lung cancer; $\Delta\psi m$: mitochondrial membrane potential; LD50: the median lethal dose; IC50: 50% inhibiting concentration; TCGA: The Cancer genome atlas; i.v.: intravenous administration; p.o.: oral administration. AR: androgen receptor; RFA1: replication factor A protein 1.

Declarations

Acknowledgement

None.

Funding

This work was supported by Natural Science Foundation of China (21877049), National Program for Support of Top-notch Young Professionals (W02070191), Major Program for Tackling Key Problems of

Industrial Technology in Guangzhou (201902020013), Dedicated Fund for Promoting High-Quality Marine Economic Development in Guangdong Province (GDOE-2019-A31), and Guangzhou Key Laboratory of Molecular and Functional Imaging for Clinical Translation (Project No. 201905010003).

Availability of data and materials

The expression of TRPM8 and AR in human normal lung tissues and lung cancer cells are obtained from TCGA data base (http://ualcan.path.uab.edu/cgi-bin/ualcan-res.pl). The relationship of expression of TRPM8 and patient survival rate was obtained from PROGgene data base (http://genomics.jefferson.edu/proggene/). All other data are available in the main text or the supplementary materials.

Authors' contributions

Conception and design: Haoqiang Lai, Tianfeng Chen and An Hong. Development of methodology: Haoqiang Lai and Tianfeng Chen. Writing, review, and/or revision of the manuscript: Haoqiang Lai, Tianfeng Chen and An Hong. Wenwei Lin carried out the experiments of MTT assay. Chang Liu examined the *in vivo* anticancer assay. All authors reviewed and approved the final manuscript.

Ethics approval

The animal experiment was approved by the Animal Experimentation Ethics Committee of Jinan University.

Consent for publication

All authors have agreed to publish this manuscript.

Competing Interest

The authors declare that they have no competing interests.

Author details

[a] Department of Cell Biology & Institute of Biomedicine, National Engineering Research Center of Genetic Medicine, Guangdong Provincial Key Laboratory of Bioengineering Medicine, College of Life Science and Technology, Jinan University, Guangzhou, 510632, China. [b] Department of Chemistry, Jinan University, Guangzhou, 510632, China.

References

1. Gridelli C, Rossi A, Carbone DP, Guarize J, Karachaliou N, Mok T, Petrella F, Spaggiari L, Rosell R: Non-small-cell lung cancer. Nat. Rev. Dis. Primers. 2015, 1:15009.

2. Torre LA, Siegel RL, Jemal A: Lung cancer statistics. In Lung cancer and personalized medicine. Springer; 2016: 1-19
3. Goldstraw P, Ball D, Jett JR, Le Chevalier T, Lim E, Nicholson AG, Shepherd FA: Non-small-cell lung cancer. The Lancet. 2011, 378:1727-40.
4. Otani S, Sasaki J, Masuda K, Okamoto K, Namubu A, Matsumoto T, Tanaka M, Ishihara M, Nakahara Y, Fukui T: Synergistic anti-tumor effect of the combination of amrubicin and erlotinib in non-small cell lung cancer with wild type. Cancer Res 76(14 Suppl):Abstract nr 2284; 2016. http://doi.10.1158/1538-7445.
5. Deng S, Yan T, Jendrny C, Nemecek A, Vincetic M, Gödtel-Armbrust U, Wojnowski L: Dexrazoxane may prevent doxorubicin-induced DNA damage via depleting both topoisomerase II isoforms. BMC cancer. 2014, 14:842.
6. Mo J, He L, Ma B, Chen T: Tailoring particle size of mesoporous silica nanosystem to antagonize glioblastoma and overcome blood–brain barrier. ACS Appl Mater Inte. 2016, 8:6811-25.
7. Seebacher NA, Richardson DR, Jansson PJ: A mechanism for overcoming P-glycoprotein-mediated drug resistance: novel combination therapy that releases stored doxorubicin from lysosomes via lysosomal permeabilization using Dp44mT or DpC. Cell Death Dis. 2016, 7:e2510.
8. Kartal-Yandim M, Adan-Gokbulut A, Baran Y: Molecular mechanisms of drug resistance and its reversal in cancer. Crit. Rev. Biotechnol. 2016, 36:716-26.
9. Xu F, Wang F, Yang T, Sheng Y, Zhong T, Chen Y: Differential drug resistance acquisition to doxorubicin and paclitaxel in breast cancer cells. Cancer Cell Int. 2014, 14:538.
10. Wijdeven RH, Pang B, van der Zanden SY, Qiao X, Blomen V, Hoogstraat M, Lips EH, Janssen L, Wessels L, Brummelkamp TR: Genome-wide identification and characterization of novel factors conferring resistance to topoisomerase II poisons in cancer. Cancer Res. 2015, 19:4176-4187.
11. Hirsch FR, Suda K, Wiens J, Bunn Jr PA: New and emerging targeted treatments in advanced non-small-cell lung cancer. The Lancet. 2016, 388:1012-24.
12. Vinod B, Antony J, Nair H, Puliyappadamba V, Saikia M, Narayanan SS, Bevin A, Anto RJ: Mechanistic evaluation of the signaling events regulating curcumin-mediated chemosensitization of breast cancer cells to 5-fluorouracil. Cell Death Dis. 2013, 4:e505.
13. Trigo JM, Leary A, Besse B, Ponce DCS, Arrondeau J, Moreno V, Doger B, López RL, Awada A, Jungels C: Efficacy and safety of lurbinectedin (PM1183, Zepsyre®) in small cell lung cancer (SCLC): results from a phase 2 study. J Clin Oncol. 2018, 36. http://doi:10.1200/JCO.2018.36.15_suppl.8570.
14. Chen S-R, Dai Y, Zhao J, Lin L, Wang Y, Wang Y: A Mechanistic Overview of Triptolide and Celastrol, Natural Products from Tripterygium wilfordii Hook F. Front Pharmacol, 2018, 9.
15. Ackermann A, Karagoez AC, Ghoochani A, Buchfelder M, Eyuepoglu I, Tsogoeva SB, Savaskan N: Cytotoxic profiling of artesunic and betulinic acids and their synthetic hybrid compound on neurons and gliomas. Oncotarget. 2017, 8:61457-74.
16. Noel P, Von Hoff DD, Saluja AK, Velagapudi M, Borazanci E, Han H: Triptolide and Its Derivatives as Cancer Therapies. Trends Pharmacol Sci. 2019, 40:327-41.

17. Su J, Lai H, Chen J, Li L, Wong Y-S, Chen T, Li X: Natural borneol, a monoterpenoid compound, potentiates selenocystine-induced apoptosis in human hepatocellular carcinoma cells by enhancement of cellular uptake and activation of ROS-mediated DNA damage. PLoS One. 2013, 8:e63502.
18. Chen J, Li L, Su J, Li B, Zhang X, Chen T: Proteomic analysis of G2/M arrest triggered by natural borneol/curcumin in HepG2 cells, the importance of the reactive oxygen species-p53 pathway. J Agr Food Chem. 2015, 63:6440-49.
19. Chen J, Li L, Su J, Li B, Chen T, Ling F, Zhang X: Enhancing effect of natural borneol on the cellular uptake of demethoxycurcumin and their combined induction of G2/M arrest in HepG2 cells via ROS generation. J Func Foods. 2015, 17:103-14.
20. Yin Y, Cao L, Ge H, Duanmu W, Tan L, Yuan J, Tunan C, Li F, Hu R, Gao F: L-Borneol induces transient opening of the blood–brain barrier and enhances the therapeutic effect of cisplatin. Neuroreport. 2017, 28:506-13.
21. Losko M, Dolicka D, Pydyn N, Jankowska U, Kedracka-Krok S, Kulecka M, Paziewska A, Mikula M, Major P, Winiarski M, et al: Integrative genomics reveal a role for MCPIP1 in adipogenesis and adipocyte metabolism. Cell Mol Life Sci. 2019, http://doi.10.1007/s00018-019-03434-5.
22. Wang F-X, Luo Y-M, Ye Z-Q, Cao X, Liang J-N, Wang Q, Wu Y, Wu J-H, Wang H-Y, Zhang M, et al: iTRAQ-based proteomics analysis of autophagy-mediated immune responses against the vascular fungal pathogen Verticillium dahliae in Arabidopsis. *Autophagy* 2018, 14:598-618.
23. Fathi F, Rezabakhsh A, Rahbarghazi R, Rashidi M-R: Early-stage detection of VE-cadherin during endothelial differentiation of human mesenchymal stem cells using SPR biosensor. Bios Bioelectron. 2017, 96:358-66.
24. Tyagi D, Perez JB, Nand A, Cheng Z, Wang P, Na J, Zhu J: Detection of embryonic stem cell lysate biomarkers by surface plasmon resonance with reduced nonspecific adsorption. Ana Biochem. 2015, 471:29-37.
25. Lai H, Fu X, Sang C, Hou L, Feng P, Li X, Chen T: Selenadiazole Derivatives Inhibit Angiogenesis-Mediated Human Breast Tumor Growth by Suppressing the VEGFR2-Mediated ERK and AKT Signaling Pathways. Chem Asian J. 2018, 13:1447-57.
26. Buondonno I, Gazzano E, Jean SR, Audrito V, Kopecka J, Fanelli M, Salaroglio IC, Costamagna C, Roato I, Mungo E: Mitochondria-targeted doxorubicin: a new therapeutic strategy against doxorubicin-resistant osteosarcoma. Mol Cancer Ther. 2016, 15:2640-52.
27. Zhao J-y, Lu Y, Du S-y, Song X, Bai J, Wang Y: Comparative pharmacokinetic studies of borneol in mouse plasma and brain by different administrations. J Zhejiang Univ-Sc B. 2012, 13:990-96.
28. Commission CP: People's Republic of China Pharmacopoeia. *Beijing:* The Medicine Science and Technology Press of China 2015.
29. You Y, He L, Ma B, Chen T: High-Drug-Loading Mesoporous Silica Nanorods with Reduced Toxicity for Precise Cancer Therapy against Nasopharyngeal Carcinoma. Adv Funct Mater. 2017, 27:1703313.

30. Guo H, Jin H, Gui R, Wang Z, Xia J, Zhang F: Electrodeposition one-step preparation of silver nanoparticles/carbon dots/reduced graphene oxide ternary dendritic nanocomposites for sensitive detection of doxorubicin. Sensor Actuat B-Chem. 2017, 253:50-57.
31. Poornima P, Kumar VB, Weng CF, Padma VV: Doxorubicin induced apoptosis was potentiated by neferine in human lung adenocarcima, A549 cells. Food Chem Toxicol. 2014, 68:87-98.
32. Schmitt AM, Garcia JT, Hung T, Flynn RA, Shen Y, Qu K, Payumo AY, Peres-da-Silva A, Broz DK, Baum R, et al: An inducible long noncoding RNA amplifies DNA damage signaling. Nat Genet. 2016, 48:1370-76.
33. Song Z, Chang Y, Xie H, Yu X-F, Chu PK, Chen T: Decorated ultrathin bismuth selenide nanosheets as targeted theranostic agents for in vivo imaging guided cancer radiation therapy. NPG Asia Mater. 2017, 9:e439.
34. Chang Y, He L, Li Z, Zeng L, Song Z, Li P, Chan L, You Y, Yu X-F, Chu PK: Designing core–shell gold and selenium nanocomposites for cancer radiochemotherapy. Acs Nano. 2017, 11:4848-58.
35. Anders U, Schaefer JV, Hibti F-E, Frydman C, Suckau D, Plückthun A, Zenobi R: SPRi-MALDI MS: characterization and identification of a kinase from cell lysate by specific interaction with different designed ankyrin repeat proteins. Anal Bioanal Chem. 2017, 409:1827-36.
36. Braat S, Kooy RF: The GABA(A) Receptor as a Therapeutic Target for Neurodevelopmental Disorders. Neuron. 2015, 86:1119-30.
37. Hantute-Ghesquier A, Haustrate A, Prevarskaya N: TRPM family channels in cancer. Pharmaceuticals. 2018, 11:58.
38. Goswami CP, Nakshatri H: PROGgeneV2: enhancements on the existing database. Bmc Cancer. 2014, 14. http://doi.10.1186/1471-2407-14-970.
39. Chandrashekar DS, Bashel B, Balasubramanya SAH, Creighton CJ, Ponce-Rodriguez I, Chakravarthi BVSK, Varambally S: UALCAN: A Portal for Facilitating Tumor Subgroup Gene Expression and Survival Analyses. Neoplasia. 2017, 19:649-58.
40. Nazıroğlu M, Blum W, Jósvay K, Çiğ B, Henzi T, Oláh Z, Vizler C, Schwaller B, Pecze L: Menthol evokes Ca^{2+} signals and induces oxidative stress independently of the presence of TRPM8 (menthol) receptor in cancer cells. Redox Biol. 2018, 14:439-49.
41. Liu Y, Luo Y, Li X, Zheng W, Chen T: Rational Design of Selenadiazole Derivatives to Antagonize Hyperglycemia-Induced Drug Resistance in Cancer Cells. Chemistry Asian J. 2015, 10:642-52.
42. Fulda S: Targeting apoptosis for anticancer therapy. Semin Cancer Biol. 2015: 84-88.
43. Zhao Z, Gao P, You Y, Chen T: Cancer-Targeting Functionalization of Selenium-Containing Ruthenium Conjugate with Tumor Microenvironment-Responsive Property to Enhance Theranostic Effects. Chem Europ J. 2018, 24:3289-98.
44. Mizumachi H, Yoshida S, Tomokiyo A, Hasegawa D, Hamano S, Yuda A, Sugii H, Serita S, Mitarai H, Koori K, et al: Calcium-sensing receptor-ERK signaling promotes odontoblastic differentiation of human dental pulp cells. Bone. 2017, 101:191-201.

45. Ghigo A, Laffargue M, Li M, Hirsch E: PI3K and Calcium Signaling in Cardiovascular Disease. Circ Res. 2017, 121:282-92.
46. Ghosh J, Das J, Manna P, Sil PC: The protective role of arjunolic acid against doxorubicin induced intracellular ROS dependent JNK-p38 and p53-mediated cardiac apoptosis. Biomaterials. 2011, 32:4857-66.
47. Aubrey BJ, Kelly GL, Janic A, Herold MJ, Strasser A: How does p53 induce apoptosis and how does this relate to p53-mediated tumour suppression? Cell Death Different. 2018, 25:104.
48. Soriani A, Iannitto ML, Ricci B, Fionda C, Malgarini G, Morrone S, Peruzzi G, Ricciardi MR, Petrucci MT, Cippitelli M, Santoni A: Reactive Oxygen Species- and DNA Damage Response-Dependent NK Cell Activating Ligand Upregulation Occurs at Transcriptional Levels and Requires the Transcriptional Factor E2F1. J Immunol. 2014, 193:950-60.
49. Wang S, Zhang D, Hu J, Jia Q, Xu W, Su D, Song H, Xu Z, Cui J, Zhou M, et al: A clinical and mechanistic study of topical borneol-induced analgesia. Embo Mol Med. 2017, 9:802-15.
50. Shuck SC, Turchi JJ: Targeted Inhibition of Replication Protein A Reveals Cytotoxic Activity, Synergy with Chemotherapeutic DNA-Damaging Agents, and Insight into Cellular Function. Cancer Res. 2010, 70:3189-98.

Additional Files

Additional file1: Table. s1 Acute oral toxicity evaluation of synthetic borneol and natural borneol ((+)-borneol).

Additional file2: Fig. s1 Histological analysis of stomach, intestinum tenue, liver, spleen and lung of SD rats treated with synthetic borneol and nature borneol ((+)-borneol) at 5 g/kg.

Additional file3: Table. s2 Growth inhibition of the combination treatment of chemotherapeutic agents and NB against A549 cells.

Additional file4: Fig. s2 Effects of NB combined with DOX on mitochondria membrane depolarization by staining with JC-1(2 μM). Bars with * is represented as statistically different at $P<0.05$.

Additional file5: Fig. s3. NB sensitizes DOX induced killing capacity is independent of androgen receptor (AR) mediated pathway. **a** Protein expression level of AR after the introduction of short interfering double-stranded RNAs (siRNAs). **b** Effects of the anticancer efficiency of NB and DOX combination treatment in AR knock down cells.

Additional file 6: Raw image files of western blots.

Figures

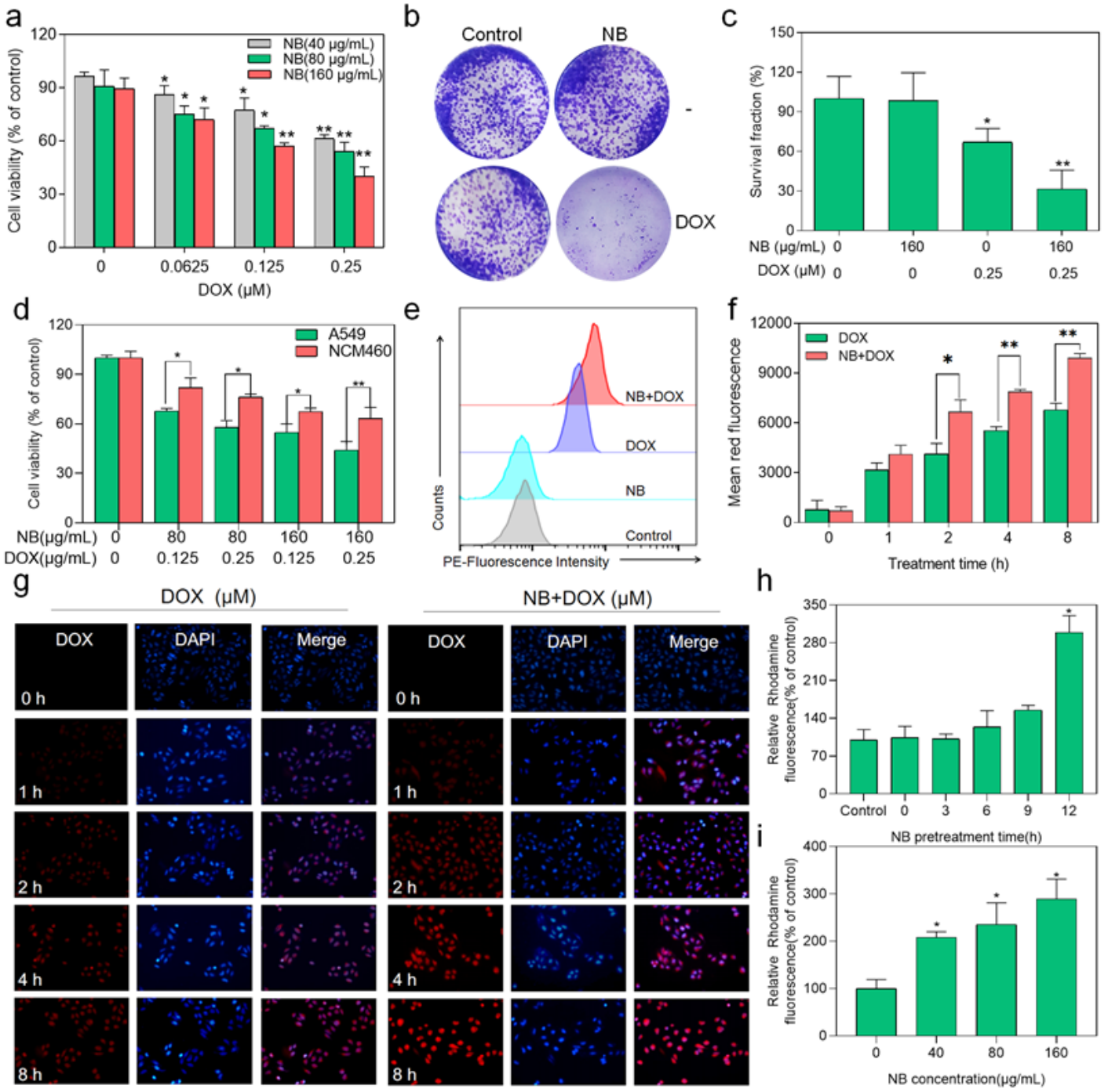

Figure 1

NB augments the cell growth inhibitory effects of DOX against A549 cells through enhancing the cellular uptake of DOX. a NB enhanced DOX-mediated killing against A549 cells in a dose-dependent manner. b-c NB augmented the suppression effect of DOX on the long term clonogenic assay. * and ** are represented as P<0.05 and P<0.001 versus the untreated control groups, respectively. d Growth inhibition of the combination treatment of NB and DOX in NCM-460 cells. e Flow cytometric histogram of DOX cellular accumulation. f Representative of mean red fluorescence of DOX in A549 cells. g Representative fluorescence images of the intracellular uptake of DOX in A549 cells. NB inhibited P-gp function in a

concentration h and time dependent manner i * and ** are described as statistically different at the P < 0.05 and P<0.001.

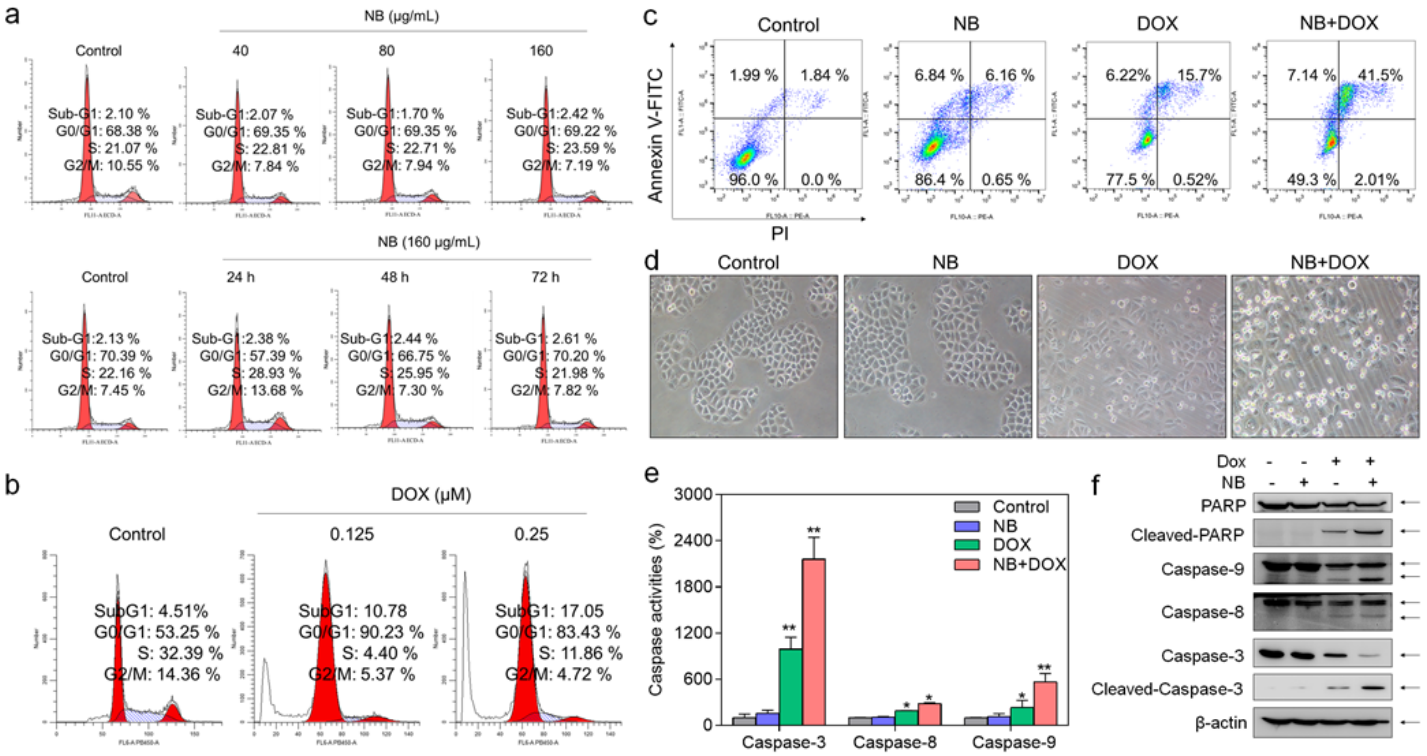

Figure 2

NB potentiates DOX-induced A549 cells apoptosis. a Effects of NB on the cell cycle distribution of A549 cells. b Effects of DOX on the cell cycle distribution of A549 cells. c Pretreatment of NB enhances DOX-induced apoptosis in A549 cells. d Representative images of A549 cells after the treatment of NB and DOX. e Activation of Caspase-3, caspase-8 and caspase-9 induced by the combination treatment of NB and DOX. Briefly, incubation of 100 μg protein with 5 μL specific fluorescent substrates for caspase-3/-8/-9 for 2 h and then the fluorescence was measured by Biotek Microplate System. f Western blotting assay of the protein expression level of caspase-3/-8/-9, PARP, cleaved-PARP, and cleaved-caspase-3. * and ** are denoted as significant difference at P < 0.05 and P < 0.01.

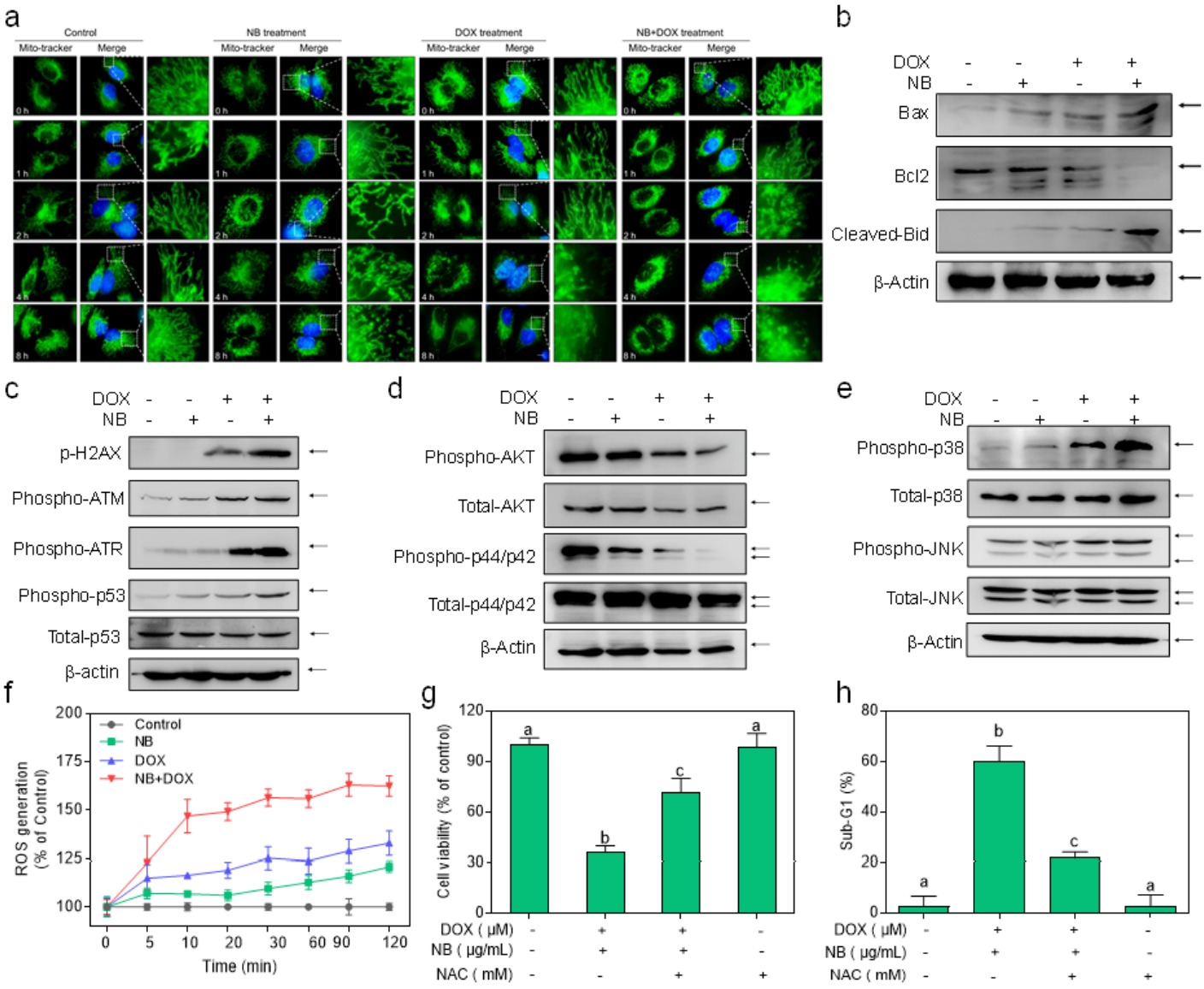

Figure 3

NB and DOX synergize to activate ROS-mediated pathways in A549 cells. a Alternation of mitochondrial structure induced by the combined treatment of NB and DOX in A549 cells (magnification, 1000×). b Protein expression of Bcl-2, Bax and truncation of Bid after the incubation of NB and DOX in A549 cells. c NB enhances DOX-induced ROS production in A549 cells. The combination treatment of NB and DOX suppresses phosphorylated-AKT and -ERK d, while upregulates the expression level of phosphor-p38MAPK and phosphor-JNK e. f NB potentiates DOX-induced phosphorylation of ATM, ATR, p53, and histone. g NAC pretreatment elevates the cell viability induced by the combination treatment of NB and DOX. h NAC reduces apoptosis inducing capacity of NB and DOX. Cells were treated with 5 mM NAC for 2 h prior to incubate with NB and DOX. Three independent experiments were carried out for this assay. Bars with different characters (a–c) are denoted as statistical difference at $P<0.05$.

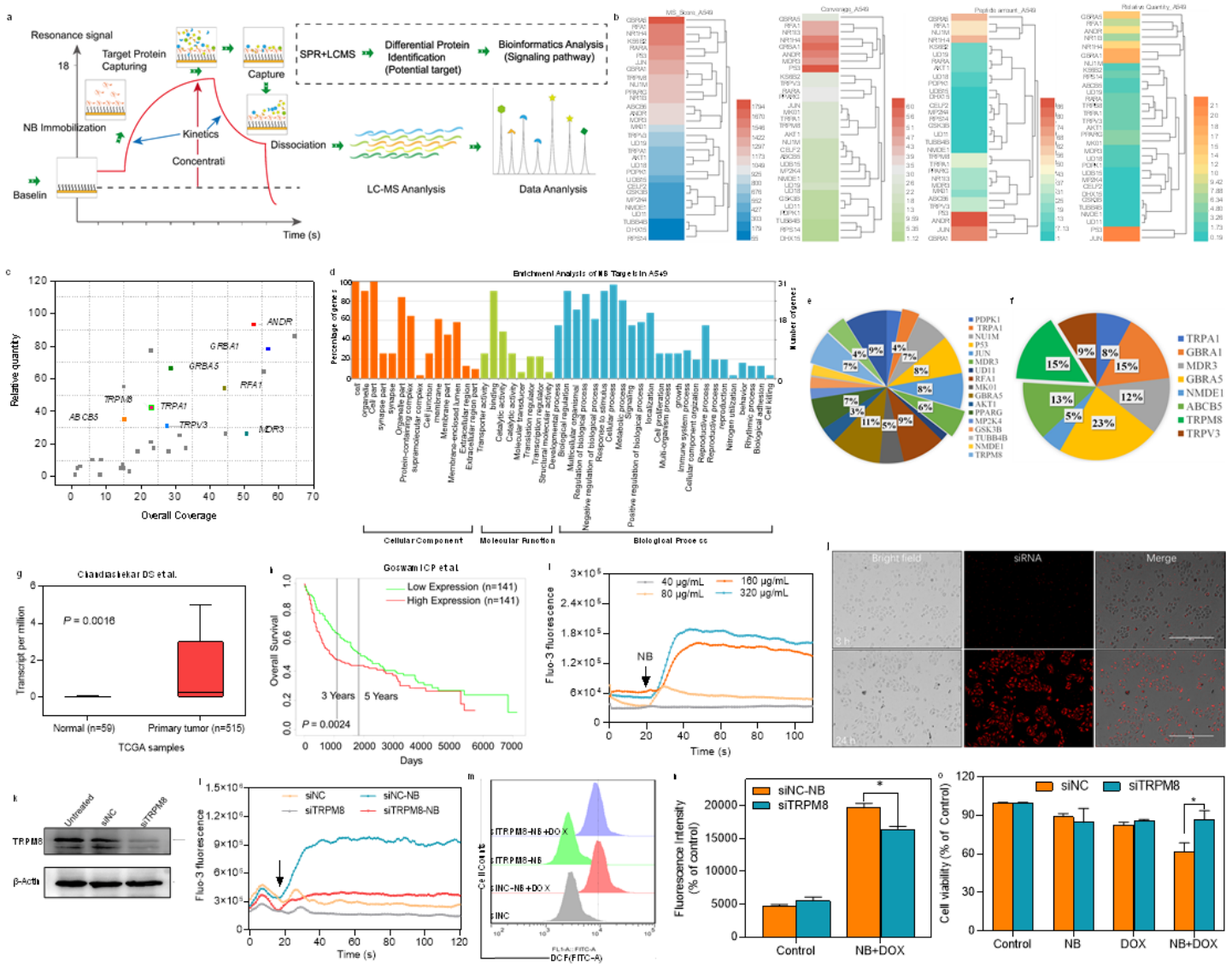

Figure 4

TRPM8-mediated Ca2+ mobilization contributes to the synergism of NB and DOX. a Scheme of MS-SPRi technique for the screen of candidate protein target of NB. b MS score and relative quantity of target proteins captured by NB. c The captured proteins were displayed in scatterplots. d Go analysis of the captured proteins of A549 cells. e Enrichment analysis of captured targets in response to stress e and transmembrane transporter activity f. g Different expression level of TRPM8 between human normal lung tissue and lung cancer tissue. The data comes from TCGA database [39] (http://ualcan.path.uab.edu/). h The relationship between the expression of TRPM8 in human lung cancer and the survival rate of patients. The data comes from PROGene database [38] (http://genomics.jefferson.edu/proggene/). i NB evokes Ca2+ concentration changes in the cytoplasmic. Representative images of cells transfected with siRNA of TRPM8 j and TRPM8 expression of transfected cells k. l Intracellular Ca2+ accumulation triggered by NB (160 μg/mL) in TRPM8 knockdown cells. Intracellular ROS accumulation m and fluorescence intensity of DCF n induced by NB and DOX combined treatment in TRPM8 knockdown cells. o Genetically knock down of TRPM8 restrains the killing capacity of NB and DOX against A549 cells. Bars

with * is represented as statistically different at P<0.05. Arrow indicates the addition of indicated concentration of NB into cells.

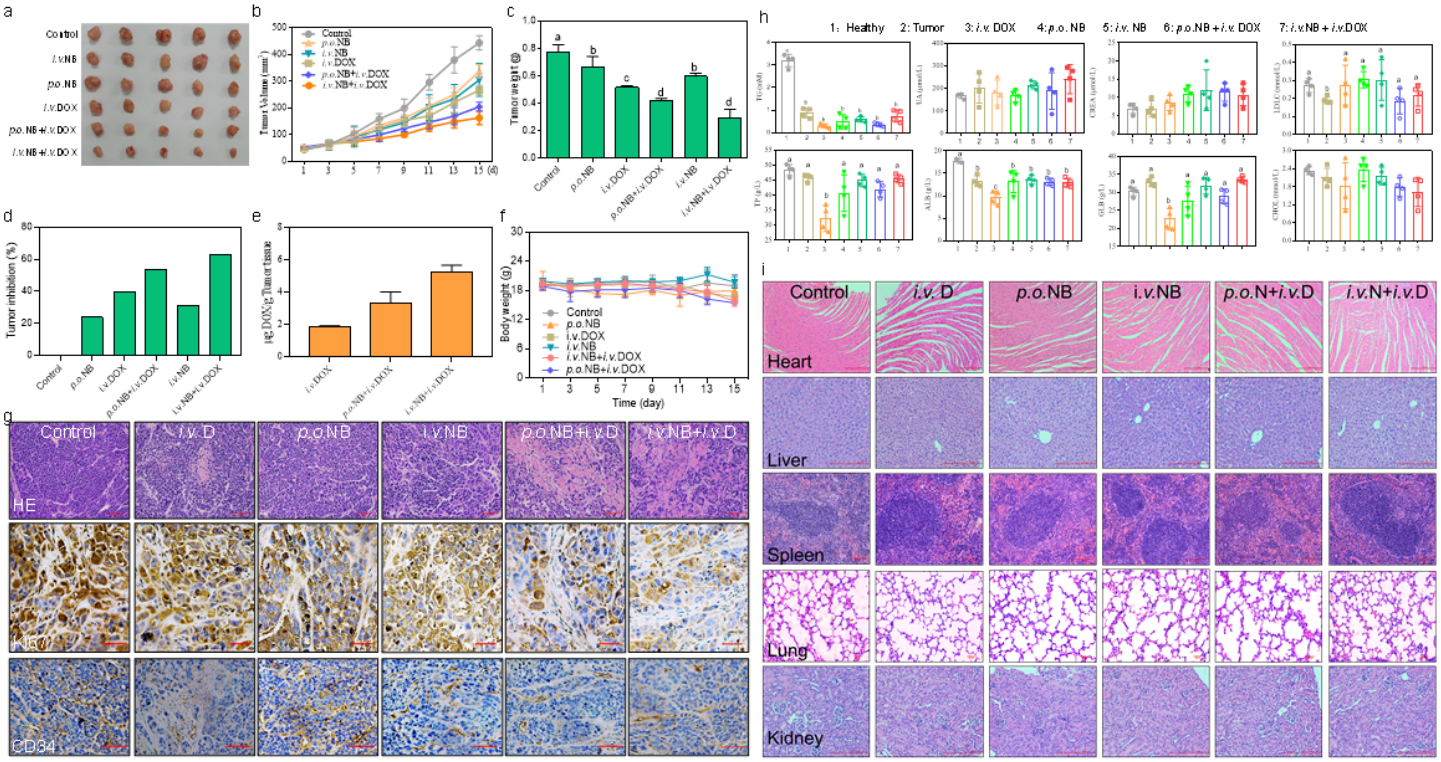

Figure 5

NB potentiates DOX antitumor activities in vivo. Representative photograph of tumors in different treated groups a. Tumor volume b and tumor weight c tumor inhibition d, DOX accumulation in tumors e and body weight f of A549 xenografts in nude mice after the treatment of saline solution, NB, DOX, and NB+DOX. g IHC and H&E staining of tumour tissues from each group. h Histological study of the combined treatment of NB and DOX. i Hematological analysis of healthy, tumor-bearing, and the combination treatment of NB and DOX in nude mice. Each value represents means ± SD. i.v.: intravenous administration; p.o.: oral administration; Bars with different characters (a–d) are statistically different at P<0.05.

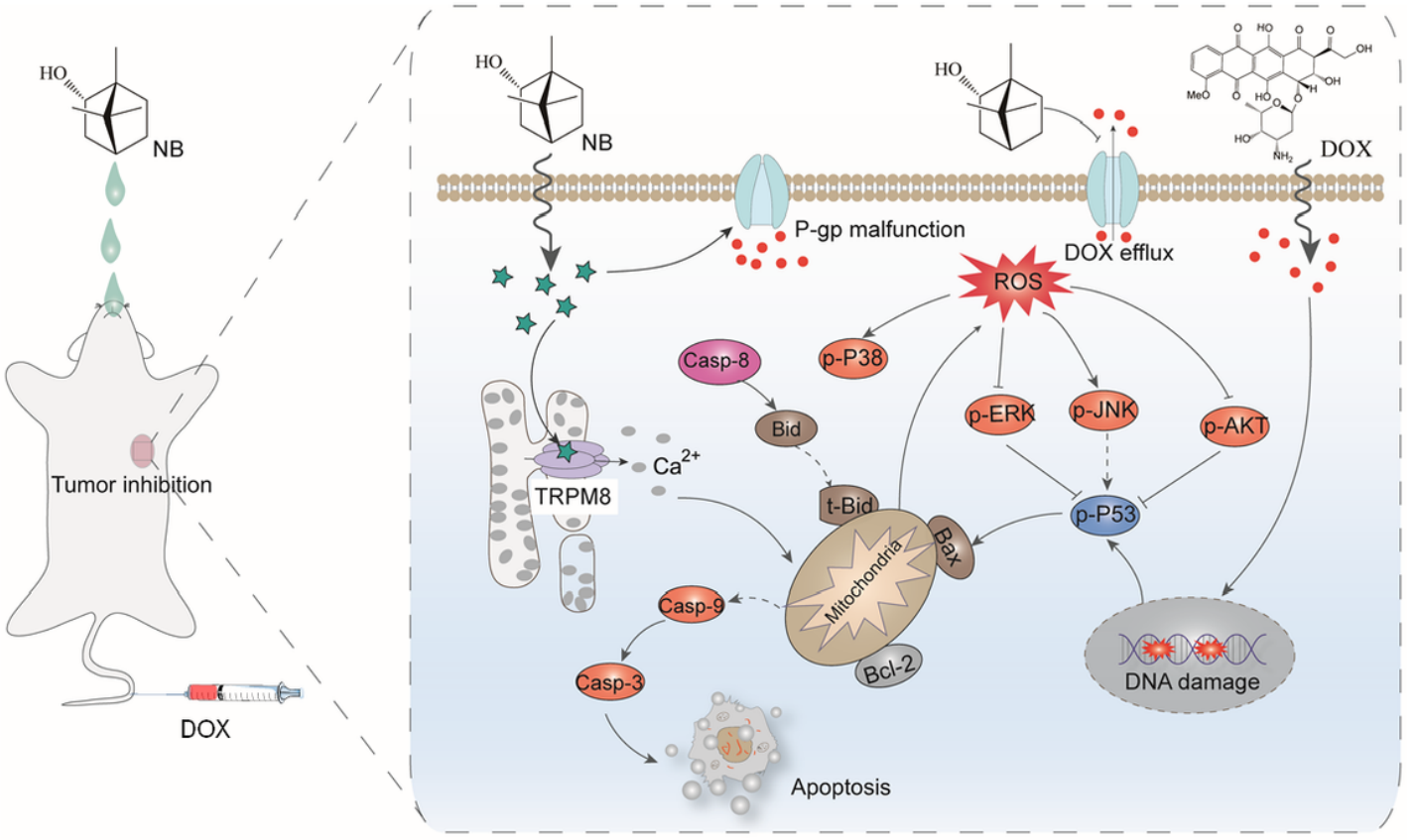

Figure 6

The proposed signaling pathway induced by the combination treatment of NB and DOX. NB enhances DOX cellular accumulation and subsequently augments DNA damage, which activates p53 pathway and result in activation of mitochondria-mediated apoptosis pathway through downregulating the expression ratio of Bcl-2/Bax. Additionally, NB also triggers intracellular Ca2+ immobilization through interacting with TRPM8. Ca2+ overproduction may facilitate mitochondria dysfunction and increase ROS generation and therefore suppresses activation of ERK1/2 and AKT, and facilitates p38MAPK and JNK phosphorylation, which thus boosts p53 activation and strengthens the apoptosis effects.

Supplementary Files

This is a list of supplementary files associated with this preprint. Click to download.

- Additionalfile1.docx
- Additionalfile4.docx
- Additionalfile2.docx
- Additionalfile3.docx
- Additionalfile5.docx

- Additionalfiles6.docx